Photoionization of the barium $6s\,6p$ $^1P^{\circ}_1$ state: Comparison of theory and experiment including hyperfine-depolarization effects

Robert P. Wood, Chris H. Greene, and Darrell Armstrong

Department of Physics and Joint Institute for Laboratory Astrophysics, University of Colorado, Boulder, Colorado 80309-0440

(Received 30 March 1992; revised manuscript received 12 June 1992)

Recent experimental studies of the photoionization cross section of excited barium are compared with detailed R-matrix calculations, carried out in the energy range between the Ba$^+$ $6s$ and $5d_{3/2}$ thresholds. The study sheds light on existing discrepancies between theory and experiment, showing in particular that many of them derive from hyperfine-induced mixing of magnetic substates M_J. Experimental measurements shown here confirm this effect. Except for discrepancies in the shape of a few resonance features, generally good agreement is now obtained between experiment and theory.

PACS number(s): 32.80.Fb, 31.20.Tz, 31.10.+z

I. INTRODUCTION

While photoionization experiments and theory were focused for decades on understanding the spectra of ground-state atoms, excited-state photoionization has been increasingly investigated in recent years. A major test case for experimental techniques and theoretical descriptions has proved to be the photoionization of the $6s\,6p$ $^1P^{\circ}_1$ level of atomic barium. The past few years have seen an explosion in the number of experimental [1–6] and theoretical [7–10] papers devoted to this specific system. Some earlier experimental work [11,12] treating photoionization of the $6s\,6p$ $^1P^{\circ}_1$ state was concerned more with photoelectron angular distributions and dealt with only one (or a few) wavelengths, and will not be analyzed in detail here. Similarly, the earliest theoretical descriptions at the independent-electron level (e.g., Ref. [13]) are largely ignored in the discussion that follows, because the strong electron correlations render this approximation virtually useless in the energy range being considered.

The first experiments [1,2] attempted primarily to set the *scale* of the total photoionization cross section of this excited state of barium. The study of Kallenbach, Kock, and Zierer [1] introduced a new technique which apparently overestimated the size of the cross section by about a factor of 5, based on subsequent theoretical [7–10] and experimental [3,4] efforts. Three papers [4–6] have measured the *shape* of the photoionization spectrum versus the energy of the photoionizing laser, showing complex autoionizing resonance structures between the $6s$ and $5d$ thresholds. The extensive mapping of resonance structures over a wide energy range, and for different laser polarizations, by Lange, Eichmann, and Sandner [5] has provided in particular a benchmark measurement which should allow the most detailed comparison with theory yet available. This measurement has shown, for instance, a problem with the calculation of Bartschat and McLaughlin [7], which fails to give a major feature: the $6p^2\,^1S_0$ autoionizing "complex resonance" near the wavelength 370 nm of the photoionizing

laser. On the other hand, the jj-coupled eigenchannel R-matrix calculations of Refs. [8,9] give a realistic description of this strong feature.

It has been pointed out previously [4,5] that the agreement between experiment and theory [9,10] has been less than satisfactory, especially in the resonance peak heights. The purpose of the present study is to give a detailed comparison between the experiment of Lange, Eichmann, and Sandner [5] and our calculations, in order to examine in more detail the range of applicability of the eigenchannel R-matrix approach and its limitations. In doing this we have uncovered a number of important aspects which are essential for a complete understanding of these measurements. The most important of these is the key role of *hyperfine structure* in modifying the polarization-scheme-dependent selection rules presented, e.g., in Ref. [4]. Additional evidence supporting our interpretation is presented in the form of new experimental measurements.

II. EVIDENCE FOR HYPERFINE DEPOLARIZATION AND ITS DESCRIPTION

Our calculations use the eigenchannel R-matrix approach in combination with multichannel quantum-defect theory (MQDT), as described in detail elsewhere [9]. The entire calculation is performed in jj coupling, which was shown in Ref. [9] to give marginally better agreement with experiment than does the LS-coupled calculation followed by a recoupling frame transformation. We have modestly extended the calculation of Refs. [8,9] by increasing the size of the R-matrix box to $r_0 = 22$ a.u. and by using approximately a 20% larger basis set. Both of these changes were seen to have little effect on the spectra calculated in Refs. [8,9]. The present calculations were performed using an energy mesh that is substantially more dense than that used in Refs. [8,9] in order to describe the true strength of narrow resonances more adequately, including a convolution over the wavelength resolution 0.2 cm^{-1} of the photoionizing laser used in the

experiment of Ref. [5]. The experimental cross sections in Ref. [5] were measured with two lasers. The first (exciting) laser at 553.7 nm was used to populate the $6s\,6p$ $^1P_1^\circ$ state and the second (photoionizing) laser was tuned to reach final-state energies between the Ba^+ $6s$ and $5d_{3/2}$ thresholds. Both lasers were linearly polarized, with the polarization vectors of the two lasers being either parallel or perpendicular in two different sets of measurements. In the parallel case the allowed final states are $J_f = 0$ or 2, $M_{J_f} = 0$, while in the perpendicular case the allowed symmetries are $J_f = 1$ or 2, $|M_{J_f}| = 1$, if we pick our quantization axis to coincide with the axis of linear polarization of the first laser. The selection of laser polarizations in the excitation scheme thus allows the experiments to probe different final-state symmetries, permitting a stringent test of the theory. A visual comparison of the theoretical spectra calculated for $J_f = 0,1,2$ in Refs. [8,9] shows that some $J_f = 1$ theoretical lines are present in the experimental "parallel" spectra of Ref. [5], which should be forbidden based on the electronic selection rule. Similarly, some $J_f = 0$ lines appear in the experimental perpendicular spectra of Ref. [5], in apparent contradiction to this electronic selection rule. We now show how hyperfine interactions can cause this breakdown of the electronic selection rules, and permit a quantitative understanding of the strength of this breakdown. It is important to

point out that the effect of hyperfine depolarization has been mentioned previously in Ref. [6], but was not verified to the extent possible in the present work.

Natural barium consists predominantly of isotopes having two different nuclear spins. The spinless $(I = 0)$ isotopes constitute 82% while the remaining 18% of natural barium atoms are $I = \frac{3}{2}$ isotopes. The latter experience hyperfine splittings, which in classical language are associated with a precession of the electronic angular momentum **J** about the total angular momentum **F** of the atom. In the experiment of Ref. [5], the first laser cannot resolve the different hyperfine levels E_F, since a pulsed dye laser of resolution 1 cm^{-1} was used to excite the $6s\,6p$ $^1P_1^\circ$ state, whose hyperfine splittings $|E_F - E_{F'}|$ are in the range 100–500 MHz [17]. Under these circumstances we can view the first linearly polarized laser as exciting only one electronic substate $|J_e = 1, M_{J_e} = 0\rangle$, with the nuclear spins $|IM_I\rangle$ oriented randomly and initially unaffected by the photoabsorption. The total cross section for photoionization of the electronic state J_e into a continuum state of angular momentum J_f, following the resonant absorption process $J_0 \to J_e$, is derived exactly like the resonance fluorescence cross section in Refs. [18,19]. After we include the effect of hyperfine-induced mixing on the excited state, the total cross section for $J_e \to J_f$ is given by

$$\sigma^{(J_0)}(J_e \to J_f) = 9(2J_e + 1)\sigma^{(\mathrm{iso})}(J_e \to J_f)\sum_{k,q}(-1)^q E_q^k(\hat{\epsilon}_1, \hat{\epsilon}_1^*)E_{-q}^k(\hat{\epsilon}_2^*, \hat{\epsilon}_2)g^{(k)}(t)\begin{Bmatrix}1 & 1 & k \\ J_e & J_e & J_0\end{Bmatrix}\begin{Bmatrix}1 & 1 & k \\ J_e & J_e & J_f\end{Bmatrix}. \tag{1}$$

The sum over k includes all electronic multipole moments created in the excited state by the one-photon absorption, namely, $k = 0,1,2$ for the scalar, dipole, and quadrupole moments. Here $\hat{\epsilon}_1$ and $\hat{\epsilon}_2$ are the polarization vectors of the exciting and ionizing lasers, respectively, and the factors E_q^k are the corresponding polarization tensors worked out explicitly in the Appendix. $\sigma^{(\mathrm{iso})}(J_e \to J_f)$ is the "isotropic" cross section for photoionization of the excited state and is given (in a.u.) by

$$\sigma^{(\mathrm{iso})}(J_e \to J_f) = \frac{4\pi^2\alpha\omega}{3(2J_e + 1)}|\langle J_f\|r^{(1)}\|J_e\rangle|^2 ,$$

where $\langle J_f\|r^{(1)}\|J_e\rangle$ is a reduced matrix element, ω is the frequency of the second (ionizing) photon, and α is the fine-structure constant. "Isotropic" in this context means that $\sigma^{(\mathrm{iso})}(J_e \to J_f)$ is the total photoionization cross section for the channel $J_e \to J_f$ which would be calculated if the excited state $|J_e\rangle$ were randomly oriented, i.e., with a density matrix $\rho_{m_e m_e'}^{(J_e)}$ proportional to the unit matrix. The factor $g^{(k)}(t)$ contains all of the effects of the

hyperfine interactions on the excited state and is given by Refs. [14,15] as

$$g^{(k)}(t) = \sum_{F,F'}\frac{(2F+1)(2F'+1)}{(2I+1)}\cos(\omega_{FF'}t)\begin{Bmatrix}F & F' & k \\ J_e & J_e & I\end{Bmatrix}^2 .$$

$$\tag{2}$$

In the limit $t \to 0$, $g^{(k)} \approx 1$, since there is no time for any precession to occur, and in this limit the nuclear spins have no role. In the opposite limit of $\omega_{F'F}t \gg 1$, all terms in Eq. (1) with $F \neq F'$ effectively average to zero and can be neglected. The experiment of Ref. [5] appears to be closer to the second limit since the average time between excitation of the $6s\,6p$ $^1P_1^\circ$ state and its absorption of an ionizing photon is several nanoseconds. This will be referred to as the limit of *complete depolarization*. For depolarization of a $J_e = 1$ electronic state by a spin $I = \frac{3}{2}$, nucleus, the cross section for photoionization of the Ba $6s\,6p$ $^1P_1$ state by a linearly polarized photon, after being excited from the ground state by a linearly polarized photon, has the general form

$$\sigma_{\mathrm{lin}}(J_0 \to J_e \to J_f) = \sigma^{(\mathrm{iso})}(1 \to 0)\{1 + 2g_{\mathrm{av}}^{(2)}P_2(\cos\theta)\} + \sigma^{(\mathrm{iso})}(1 \to 1)\{1 - g_{\mathrm{av}}^{(2)}P_2(\cos\theta)\}$$

$$+ \sigma^{(\mathrm{iso})}(1 \to 2)\{1 + \tfrac{1}{5}g_{\mathrm{av}}^{(2)}P_2(\cos\theta)\} . \tag{3}$$

Here θ is the angle between the linear polarization vectors and $P_2(\cos\theta)$ is a Legendre polynomial. The factors $g_{\mathrm{av}}^{(k)}$

represent averages of Eq. (2) over time and over the relative isotopic abundances. In the limit of complete depolarization the averages for Ba ($J_e = 1$) are

$$g_{\mathrm{av}}^{(1)} = 0.896 \ , \quad g_{\mathrm{av}}^{(2)} = 0.864 \ . \tag{4}$$

It is interesting to note that setting the polarizers at the "magic" angle ($\theta_M = 54.7^\circ$) for linear polarization still reproduces the isotropic cross section, even in the presence of depolarization, because $P_2(\cos\theta_M) = 0$. The reason for this is that the hyperfine interaction does not destroy the cylindrical symmetry about the quantization axis (the exciting laser polarization axis), and it preserves the excited-state multipolarity k. The cross sections for two circularly polarized lasers having an angle θ between their wave vectors are similarly calculated to be

$$\sigma_{LL}(J_0 \to J_e \to J_f) = \sigma^{(\mathrm{iso})}(1 \to 0)\{1 - \tfrac{3}{2}g_{\mathrm{av}}^{(1)}P_1(\cos\theta) + \tfrac{1}{2}g_{\mathrm{av}}^{(2)}P_2(\cos\theta)\}$$

$$+ \sigma^{(\mathrm{iso})}(1 \to 1)\{1 - \tfrac{3}{4}g_{\mathrm{av}}^{(1)}P_1(\cos\theta) - \tfrac{1}{4}g_{\mathrm{av}}^{(2)}P_2(\cos\theta)\}$$

$$+ \sigma^{(\mathrm{iso})}(1 \to 2)\{1 + \tfrac{3}{4}g_{\mathrm{av}}^{(1)}P_1(\cos\theta) + \tfrac{1}{20}g_{\mathrm{av}}^{(2)}P_2(\cos\theta)\} \ . \tag{5}$$

Here the subscript L refers to left circular polarization, and the first (second) subscript labels the polarization of the exciting (ionizing) laser. For the case of copropagating lasers the cross section for one laser left-circularly polarized and one laser right-circularly polarized is found by setting $\theta = \pi$ in Eq. (5). Equations (3) and (5) are generally true provided the laser polarization is 100%, even if the limit of complete depolarization (4) is not achieved. If the degree of depolarization is uncertain, measurements made for different laser polarizations and for different θ can be performed to extract the $g_{\mathrm{av}}^{(k)}$ experimentally.

Figures 1 and 2 show our calculated photoionization spectra of the barium $6s6p$ $^1P_1^\circ$ excited state for parallel and perpendicular laser polarizations, and compare them with the experimental spectra of Lange, Eichman, and Sandner [5]. The theoretical cross section has been convolved with the experimental resolution of 0.2 cm^{-1}. The calculations are done in the limit of complete hyperfine depolarization for natural barium, using Eq. (4) for the depolarization factors in Eq. (3) to calculate the cross sections for linearly polarized lasers. Several of these "electronically forbidden" resonances are reasonably strong and are marked on Figs. 1(a) and 1(b). The parallel spectrum [Fig. 1(a)] contains about 10% of the $J = 1$ symmetry while the perpendicular spectrum [Fig. 1(b)] contains about 5% of the $J = 0$ symmetry. The classification of these resonances is described in Refs. [8,9] and especially in Refs. [20–22], and will be discussed briefly below.

Figures 1(a) and 1(b) show a surprising result that the experimental $5d_{3/2}12d_{3/2}$ $J_f = 1$ resonance near 362.76 nm appears more strongly for the "electronically forbidden" parallel spectrum than for the perpendicular spectrum where it is "electronically allowed." This reversal of the expected intensities is not reproduced by the calculation. The forbidden line is seen at approximately the correct intensity in the parallel spectrum Fig. 1(a); however, in Fig. 1(b) the theoretical cross section is more than 100 times larger than the experiment. Other conspicuous discrepancies between theory and experiment can be seen in Figs. 1 and 2. Of particular note are the very high $5d_{5/2}9d_{5/2}$ and $5d_{5/2}8d_{5/2}$ $J_f = 0$ resonances near 380.76 and 384 nm, respectively, to the left of the broad

$6p^2$ $^1S_0$ perturber centered at 372 nm. The peak intensities of the calculated cross section are given on the figure and are about a factor of 100 higher in the calculation than in the experiment.

These discrepancies led us to question whether the experimental resolution of Ref. [5] is possibly broader than the quoted value of 0.2 cm^{-1}. However, the good agreement of theory and experiment for other resonances, e.g., in Figs. 1(b) and 2(b), suggests that the quoted resolution in Figs. 1 and 2 is reasonably close to 0.2 cm^{-1} after all. The origin of the disagreement became clear after plotting the raw experimental data points on top of the theoretical spectrum, as in Fig. 3. Specifically, Fig. 3 shows that across the $5d_{5/2}8d_{5/2}$ $J_f = 0$ resonance, located near 383.8 nm, the spacing of successive energy points in the experimental data is about 3 cm^{-1} (in the wavelength range 368–418 nm). Consequently, the lowest energy scans of Ref. [5] had inadequate coverage to give a faithful representation of the resonance features narrower than 3 cm^{-1}. It is clear from Fig. 3 that the calculation is in agreement with the experimental data points, even though the calculated resonance peak is approximately 30 times higher than the experimental peak.

We caution, however, that this does not totally explain all discrepancies between theory and experiment which are visible in Figs. 1 and 2. In Fig. 2(a) a resonance near 349.54 nm appears stronger in the experimental cross section of Lange, Eichmann, and Sandner than in our calculated spectrum. The reversal of the expected intensities for the $5d_{3/2}12d_{3/2}$ $J_f = 1$ resonance also cannot be explained by insufficient density of experimental energy points, as can be seen from Figs. 4(a) and 4(b). The case of parallel polarization is displayed in Fig. 4(a), where it is apparent that the density of experimental energy points is sufficient to give a faithful reproduction of the peak height of the resonance structure. It should be noted that the density of experimental energy points was not constant over the entire region of Figs. 1 and 2, which explains why the agreement appears to be better for the $5d_{3/2}12d_{3/2}$ $J_f = 1$ resonance in Fig. 4(a) than for the $5d_{5/2}8d_{5/2}$ $J_f = 0$ resonance in Fig. 3. In Fig. 4(b) the experimental peak height for perpendicular polarization is smaller than the calculation by more than a factor of 100. This disagreement has not yet been resolved; however,

after examination of the Lu-Fano plot for $J_f = 1$ in Ref. [20] the $5d_{3/2}12d_{3/2}$ $J_f = 1$ resonance appears to be almost a pure singlet, which would suggest that the cross section should be large, giving us some confidence in the calculation. In Fig. 4(a) the calculated resonance width is approximately 0.3 cm^{-1} full width at half maximum (FWHM), which is broader than the quoted laser resolution of 0.2 cm^{-1} in the experiment of Lange, Eichmann, and Sandner [5]; however, the experimental width in Fig. 4(a) is approximately twice as broad as the calculation. This may indicate an error in the calculated resonance width, or else that the experimental resolution may not
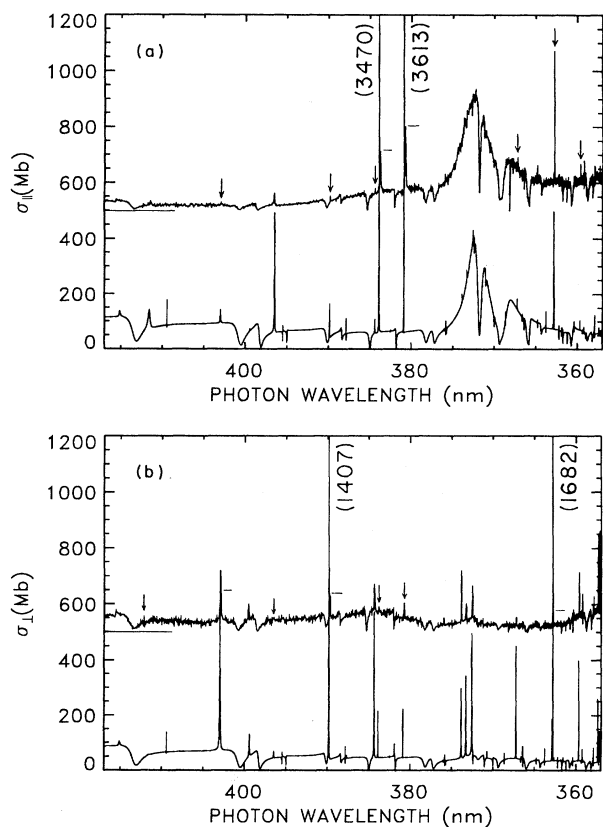
FIG. 1. Photoionization cross section of Ba $6s6p$ $^1P_1^{\circ}$ state as a function of wavelength (in vacuum) of the second laser, between the Ba$^+$ $6s$ and $5d_{3/2}$ thresholds including the effect of hyperfine depolarization in the theoretical cross sections: (a) for parallel polarization of the two lasers and (b) for perpendicular polarization of the two lasers. The experimental relative cross section of Lange, Eichmann, and Sandner [5] has been multiplied everywhere by a constant factor determined by optimizing agreement between theory and experiment in the region of the $6p^2$ ^1S resonance. The baseline of the experimental cross section has been set to 500 Mb. The calculated cross section has been convolved with the experimental resolution of 0.2 cm^{-1}. Experimental resonances which are overlapped with theory are labeled with horizontal bars. The resonances marked with the arrows are forbidden by electronic selection rules and are only present in the calculation when hyperfine effects are taken into account. Numbers in parentheses are peak intensities of theoretical cross section.
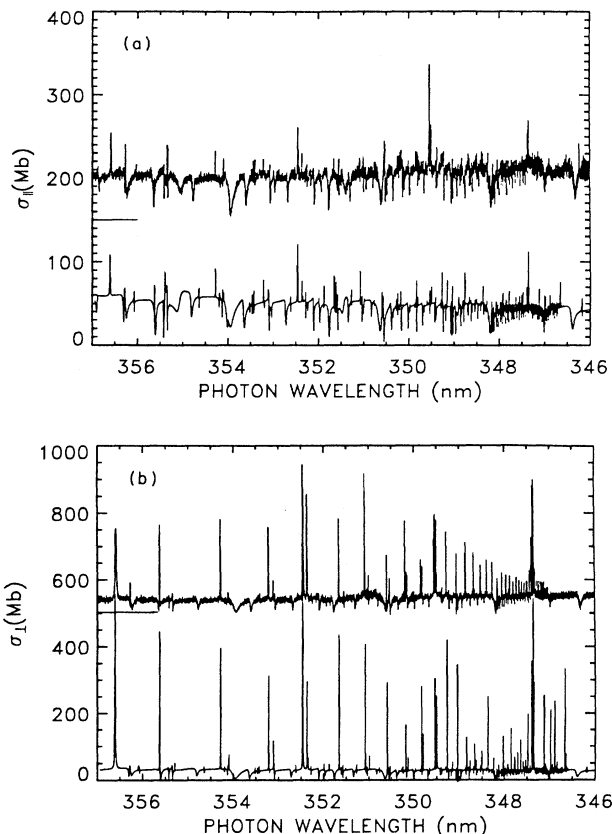
FIG. 2. Same as for Fig. 1, but at higher energies closer to and including the Ba$^+$ $5d_{3/2}$ threshold region near 346.7 nm. The baseline of the experimental cross section has been set to 150 in (a) and 500 in (b).
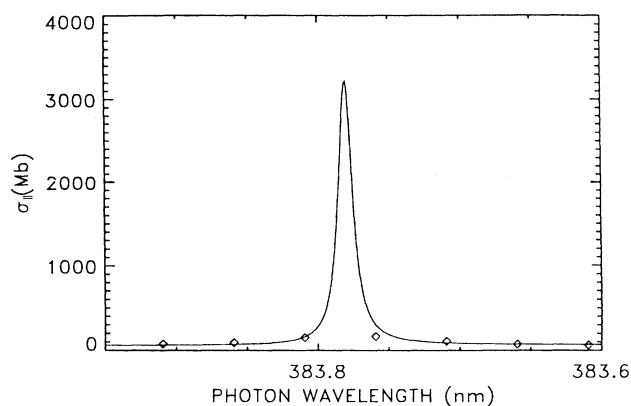
FIG. 3. Comparison of theoretical (solid curve) and experimental (open diamond) results for the $5d_{5/2}8d_{5/2}$ $J_f = 0$ resonance with parallel laser polarizers, showing that the poor agreement between theoretical and experimental peak heights stems from the insufficient density of experimental mesh points. For clarity the wavelength scale of the theoretical cross section has been shifted by approximately 0.1 nm to match the experimental resonance position for Figs. 3 and 4 only. Experimental data are from Lange, Eichmann, and Sandner [5].
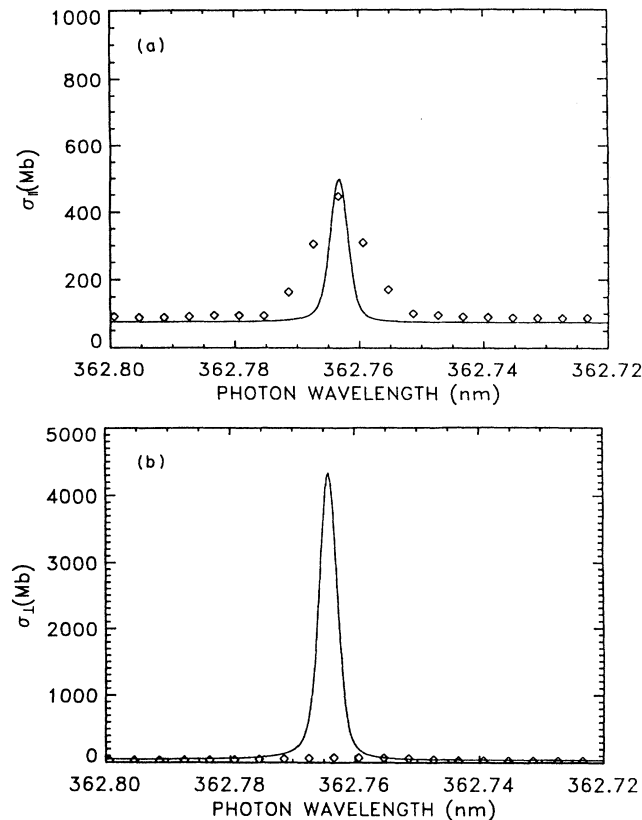
FIG. 4. Comparison of theoretical and experimental results for the $5d_{3/2}12d_{3/2}$ $J_f = 1$ resonance with lasers polarized: (a) parallel and (b) perpendicular. The theoretical wavelength scale has been shifted by approximately 0.1 nm to match the experimental resonance position. Experimental data are from Lange, Eichmann, and Sandner [5].

be as good as quoted in this wavelength range.

Another discrepancy which is particularly clear is the incorrect asymmetry of the lowest energy $J_f = 2$ resonance at 415 nm in Figs. 1(a) and 1(b), which is far more asymmetric in the measured spectrum than in the calculated spectrum. This is apparently a very sensitive case for which there is strong supporting evidence in Refs. [4,5] that the theoretical description is less than perfect. It is worth noting that the theoretical spectrum in this energy range was essentially unaffected by increases in the basis-set size and in the R-matrix box size in the present calculation compared to those of Refs. [8,9]. Yet another discrepancy is seen in the relative strength of the theoretical and experimental cross sections in Fig. 1(a) between 390 and 417 nm, with the experimental cross section apparently too small by a factor of 3–5. In this case we suspect the calculation is correct, since the independent measurement of He et al. [4] agrees better with theory than with Ref. [5].

III. INDEPENDENT DEMONSTRATION OF HYPERFINE MIXING

In order to rule out the possibility of other effects contributing to the population in the excited $|M_{J_e}| = 1$ sub-

states (e.g., stress birefringence in the cell windows or misalignment of the linear polarizers), we have performed an independent measurement of the photoionization cross section of the $6s6p$ $^1P^o_1$ state of barium in the wavelength region near the strong $5d_{3/2}8d_{3/2}$ $J_f = 1$ resonance at 402.93 nm. Nd:YAG pumped pulsed dye lasers (where Nd:YAG denotes neodymiun-doped yttrium-aluminum-garnet) with linewidths of approximately 0.5 cm^{-1} and pulse durations of 5 ns were used to excite and photoionize barium in an effusive atomic beam between two field plates in high vacuum. The exciting-laser pulse (553.7 nm) and the ionizing-laser pulse (403.4–402.45 nm) were coincident in time and the pulse energy of each laser was ≤ 10 μJ at the point of intersection with the atomic beam. The laser beams were focused to a spot size of approximately 1 mm^2. Barium ions were collected in an electron multiplier by applying a 5-V pulse to the field plates approximately 3 μs after the lasers fired. The electron multiplier output was sent to a gated integrator and boxcar averager. The analog signal from the averager was then digitized and stored in a computer for analysis.

Two measurements of the $5d_{3/2}8d_{3/2}$ $J_f = 1$ resonance were made by slowly scanning the ionizing laser from 403.4 to 402.45 nm with the laser polarization vectors set perpendicular for the first measurement and parallel for the second. For both measurements the laser light was polarized with Glan-air polarizers with a contrast ratio of 100 000:1 for a pair of crossed polarizers. To assure a reliable result for the fraction of forbidden lines, great care was taken with the parallel polarization measurement. The laser beams were first combined with a dichroic beamsplitter; then the collinear beams were sent through a linear polarizer. Parallel polarization and linear polarization of the combined beams were verified by measuring the extinction of both lasers simultaneously with a second polarizer set perpendicular to the first. The results of both parallel and perpendicular measurements of the $5d_{3/2}8d_{3/2}$ $J_f = 1$ resonance are compared in Fig. 5 to the experiment of Ref. [5] and to the present calculations performed in the limit of complete depolarization. A significant fraction of the electronically forbidden $|M_{J_e}| = 1$ substates is evident for parallel polarization in the Ref. [5] experiment, and more clearly in our new measurement. To eliminate any possibility that the $|M_{J_e}| = 1$ substates were being populated by elliptically polarized light (e.g., due to stress birefringence in the vacuum chamber entrance window), a linear polarizer was placed inside the vacuum chamber and the parallel polarization measurement was repeated. The result was identical to the earlier parallel measurement.

A ratio of the peak height on resonance (measured with respect to the structureless continuum background) for both the parallel and perpendicular scans in Fig. 5 (solid line) indicates that the fraction of $|M_{J_e}| = 1$ substates in the parallel scan is approximately 5% to 6%, or $g^{(2)}_{av} \simeq 0.92$. Since the magnitude of the parallel and perpendicular continua differ by approximately 20%, and since both continua in this experiment contain some of the electronically forbidden substates, this measurement has an uncertainty of perhaps a few percent. Nonethe-

less, the ratio is consistent with a laser-pulse duration of approximately 5 ns that is comparable to the shortest classical precession period (approximately 2 ns) of $\mathbf{J}_e$ about $\mathbf{F}$, and suggests that the hyperfine depolarization falls somewhere between the $t \rightarrow 0$ limit and the $t \rightarrow \infty$ limit of complete depolarization. In contrast, the experimental spectra of Ref. [5] show evidence of other strong forbidden lines, which is consistent with the 15-ns pulse duration of the excimer pumped dye lasers used in that experiment and closer to the limit of complete depolarization.

IV. SUMMARY

In conclusion, we have presented a detailed discussion of how hyperfine depolarization can cause a breakdown
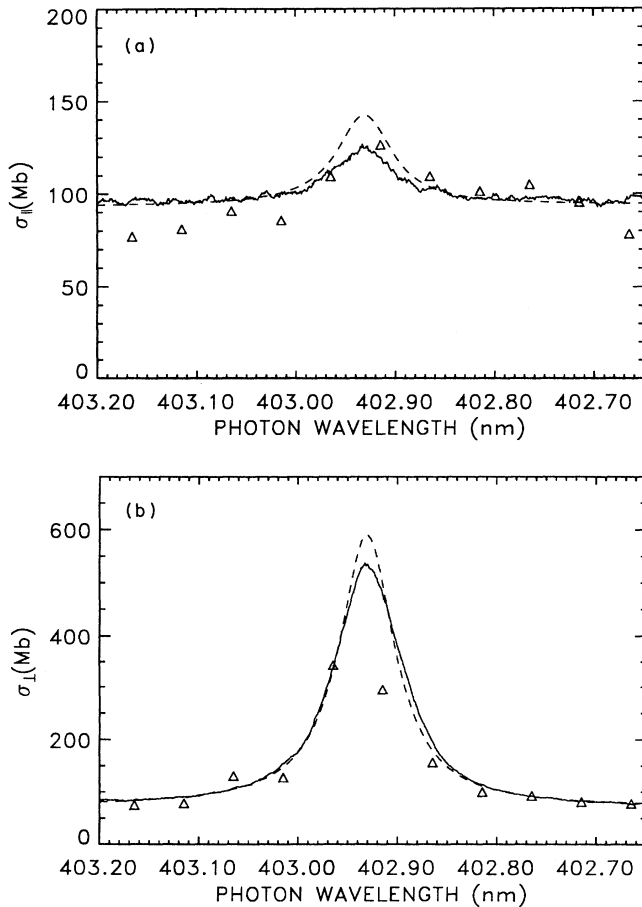
FIG. 5. Photoionization cross section in the region of the $5d_{3/2}8d_{3/2}$ $J_f = 1$ resonance: (a) parallel polarization of the two lasers; (b) perpendicular polarization of the two lasers. The dashed line is the present calculation in the limit of complete depolarization, convolved with the laser resolution of Ref. [5]. The solid line is the experimental relative cross section of the present work, and the open diamond are the data from Ref. [5]. The scales of the experimental spectra were adjusted to agree with theory near 402.75 nm. The weak appearance of the $J_f = 1$ peak in the parallel spectrum of the present work confirms the effect of hyperfine depolarization.

of the electronic selection rules, and we have calculated the size of the effect for the $6s6p$ $^1P^\circ_1$ state of barium. The calculated degree of depolarization is in good agreement with the experimental results presented. Our results are in generally good agreement with the experimental spectrum of Ref. [5] after taking into account the depolarization effect and the coarseness of the experimental energy mesh. This confirms the capability of the eigenchannel R-matrix method of Refs. [8,9] to describe the complicated interactions between numerous bound and continuum channels occurring in photoionization of excited barium. Agreement between the theoretical and experimental spectra is seen to be far better than was apparent from any of the previous experimental studies of $6s6p$ $^1P^\circ$ photoionization, although some unexplained discrepancies remain. The importance of the hyperfine interaction was appreciated by Keller, Hunter, and Berry [6] and by Refs. [14–16] and was incorporated into the theoretical description of those references. Although seemingly a small interaction, it nevertheless causes appreciable and observable effects, such as the breakdown of "electronically derived" selection rules.

ACKNOWLEDGMENTS

APPENDIX

The polarization tensors are formed by taking the following contraction of the polarization vectors:

$$E_q^k(\hat{\epsilon},\hat{\epsilon}^*) = \sum_\mu \langle 1\mu, 1q-\mu | kq \rangle \epsilon_\mu^{(1)} \epsilon_{q-\mu}^{*(1)}$$

$$= (-1)^k E_q^k(\hat{\epsilon}^*, \hat{\epsilon}) . \tag{A1}$$

Here $\langle 1\mu, 1q-\mu | kq \rangle$ is a Clebsch-Gordan coefficient and the polarization vectors have been written in terms of their spherical components, e.g., $\epsilon_0^{(1)} = \epsilon_z$, $\epsilon_{\pm1}^{(1)} = (\mp \epsilon_x - i\epsilon_y)/\sqrt{2}$. We adopt the definition of Ref. [18] for left circular polarization

$$\hat{\epsilon}_L = \frac{\hat{X}+i\hat{Y}}{\sqrt{2}} \tag{A2}$$

and right circular polarization

$$\hat{\epsilon}_R = -\frac{(\hat{X}-i\hat{Y})}{\sqrt{2}} . \tag{A3}$$

As in Ref. [19], we start from the polarization vectors in a "photon" coordinate frame whose $+\hat{z}$ axis is the photon propagation axis for circular polarization, and whose $\hat{z}$ axis is the linear polarization axis in the linear case. The only nonvanishing spherical component for left-

circularly polarized light is $\epsilon_{-1}^{(1)} = 1$, and for right circular polarization $\epsilon_{+1}^{(1)} = 1$. We find that the polarization tensors for linearly, left-circularly, and right-circularly polarized light then have nonvanishing components only for $q = 0$, for linear polarization

$$E_0^k(\hat{\epsilon}_1, \hat{\epsilon}_1^*) = \langle 10, 10 | k0 \rangle \ ,$$

for left circular polarization

$$E_0^k(\hat{\epsilon}_1, \hat{\epsilon}_1^*) = -\langle 1-1, 11 | k0 \rangle \ ,$$

and for right circular polarization

$$E_0^k(\hat{\epsilon}_1, \hat{\epsilon}_1^*) = -\langle 11, 1-1 | k0 \rangle \ .$$

The quantization axis for the ionizing photon is not in general along the same direction as that of the exciting photon, whereby the quantization axis of the ionizing photon must be rotated by an angle θ into the same frame as that of the exciting photon. Owing to the cylindrical symmetry which restricts q to zero in both photon frames, this coordinate rotation simply multiplies $E_0^k(\hat{\epsilon}_2^*, \hat{\epsilon}_2)$ by $P_k(\cos\theta)$.

[1] A. Kallenbach, M. Kock, and G. Zierer, Phys. Rev. A **38**, 2356 (1988).

[2] C. E. Burkhardt, J. L. Libbert, J. Xu, J. J. Leventhal, and J. D. Kelley, Phys. Rev. A **38**, 5949 (1988).

[3] B. Willke and M. Kock, Phys. Rev. A **43**, 6433 (1991).

[4] L. W. He, C. E. Burkhardt, M. Ciocca, J. J. Leventhal, and S. T. Manson, Phys. Rev. Lett. **67**, 2131 (1991).

[5] V. Lange, U. Eichmann, and W. Sandner, Phys. Rev. A **44**, 4737 (1991).

[6] J. S. Keller, J. E. Hunter III, and R. S. Berry, Phys. Rev. A **43**, 2270 (1991).

[7] K. Bartschat and B. M. McLaughlin, J. Phys. B **23**, L439 (1990).

[8] C. H. Greene and C. E. Theodosiou, Phys. Rev. A **42**, 5773 (1991).

[9] C. H. Greene and M. Aymar, Phys. Rev. A **44**, 6271 (1991).

[10] K. Bartschat, B. M. McLaughlin, and R. A. Hoversten, J. Phys. B **24**, 3359 (1991).

[11] S. J. Smith and G. Leuchs, Adv. At. Mol. Phys. **24**, 157 (1988).

[12] O. C. Mullins, R. Chien, J. E. Hunter III, D. K. Jordan, and R. S. Berry, Phys. Rev. A **31**, 3059 (1985).

[13] C. E. Theodosiou, Phys. Rev. A **33**, 2164 (1986).

[14] U. Fano and J. H. Macek, Rev. Mod. Phys. **45**, 553 (1973).

[15] C. H. Greene and R. N. Zare, Phys. Rev. A **25**, 2031 (1982).

[16] K. Blum, *Density Matrix Theory and Applications* (Plenum, New York, 1981).

[17] A. Lurio, Phys. Rev. **136**, A376 (1964); W. Rasmussen, R. Schieder, and H. Walther, Op. Commun. **12**, 315 (1974).

[18] R. N. Zare, *Angular Momentum* (Wiley, New York, 1988).

[19] C. H. Greene and R. N. Zare, J. Chem. Phys. **78**, 6741 (1983).

[20] M. Aymar, P. Camus, and A. El Himdy, Phys. Scr. **27**, 183 (1983).

[21] P. Camus, M. Dieulin, A. El Himdy, and M. Aymar, Phys. Scr. **27**, 125 (1983).

[22] M. Aymar, P. Camus, and A. El Himdy, J. Phys. B **15**, 759 (1982).